Control Model of Water Injection Into a Layered Formation

D. B. Silin, Lawrence Berkeley Natl. Laboratory, and **T. W. Patzek,** SPE, U. of California, Berkeley

Summary

Here we develop a new control model of water injection from a growing hydrofracture into a layered soft rock. We demonstrate that in transient flow, the optimal injection pressure depends not only on the instantaneous measurements, but also on the whole history of injection, growth of the hydrofracture, and the rock damage. Based on the new model, we design an optimal injection controller that manages the rate of water injection in accordance with hydrofracture growth and the formation properties. We conclude that maintaining the rate of water injection into a low-permeability rock above a reasonable minimum inevitably leads to hydrofracture growth, to establishment of steady-state flow between injectors and neighboring producers, or to a mixture of both. Analysis of field water injection rates and wellhead pressures leads us to believe that direct links between injectors and producers can be established at early stages of waterflood, especially if the injection policy is aggressive. Such links may develop in thin, highly permeable reservoir layers or may result from failure of the soft rock under stress exerted by injected water. These links may conduct a substantial part of injected water. Based on the field observations, we now consider a vertical hydrofracture in contact with a multilayer reservoir, where some layers have high permeability and quickly establish steady-state flow from an injector to neighboring producers.

The main result of this paper is the development of an optimal injection controller for purely transient flow, and for mixed transient/steady-state flow in a layered formation. The objective of the controller is to maintain the prescribed injection rate in the presence of hydrofracture growth and injector/producer linkage. The history of injection pressure and cumulative injection, along with estimates of the hydrofracture size, are the controller inputs. By analyzing these inputs, the controller outputs an optimal injection pressure for each injector. When designing the controller, we keep in mind that it can be used either offline as a smart adviser, or online in a fully automated regime.

Because our controller is process model-based, the dynamics of actual injection rate and pressure can be used to estimate effective area of the hydrofracture and the extent of the rock damage. The latter can be passed to the controller as one of the inputs. Finally, a comparison of the estimated fracture area with independent measurements leads to an estimate of the fraction of injected water that flows directly to the neighboring producers through links or thief-layers.

Introduction

Our ultimate goal is to design an integrated system of fieldwide waterflood surveillance and supervisory control. As of now, this system consists of the Waterflood Analyzer[1] and a network of individual injector controllers, all implemented in modular software. In the future, our system will incorporate a new generation of microelectronic/mechanical sensors (MEMS) and actuators, subsidence monitoring from satellites,[2] and other revolutionary technologies.

It is difficult to conduct a successful waterflood in a soft low-permeability rock.[3–5] On one hand, injection is slow and there is a temptation to increase the injection pressure. On the other hand, such an increase may lead to irrecoverable reservoir damage: disintegration of the formation rock and water channeling from the injectors to the producers.

In this paper, we design an optimal controller of water injection into a low-permeability rock from a growing vertical hydrofracture. The objective of control is to inject water at a prescribed rate, which may change with time. The control parameter is injection pressure. The controller is based on the optimization of a quadratic performance criterion subject to the constraints imposed by the interactions between the injection hydrofracture and the formation. The inputs include histories of wellhead injection pressure, cumulative volume of injected fluid, and hydrofracture area (**Fig. 1).** The output optimal injection pressure is determined not only by the instantaneous measurements, but also by the history of observations. With time, however, the system "forgets," so to speak, the distant past.

The wellhead injection pressures and rates are readily available if the injection water pipelines are equipped with pressure gauges and flow meters, and if the respective measurements are appropriately collected and stored as time series. It is now a common field practice to collect and maintain such data. The measurements of hydrofracture area are not as easily available. There are several techniques described in the literature. For example, Refs. 6 through 8 develop a hydraulic impedance method of characterizing injection hydrofractures. This method is based on the generation of low-frequency pressure pulses at the wellhead or beneath the injection packer, and on the subsequent analysis of the reflected acoustic waves. An extensive overview of hydrofracture diagnostics methods has been presented in Ref. 9. Theoretical background of fracture propagation was developed in Ref. 10.

The direct measurements of the hydrofracture area with currently available technologies can be expensive and difficult to obtain. We define an effective fracture area as the area of injected water-formation contact in the hydrofractured zone. Clearly, a geometric estimate of the fracture size is insufficient to estimate this effective area.

We propose a model-based identification method of the effective fracture area from the system response to the controller action. In order to implement this method, one needs to maintain a database of injection pressures and cumulative injection. As noted earlier, such databases are usually readily available and the proposed method does not impose extra measurement costs.

Earlier we proposed[4,5] a model of linear-transient, slightly compressible fluid flow from a growing hydrofracture into low-permeability, compressible rock. A similar analysis can be performed for heterogeneous layered rock. Our analysis of field injection rates and injection pressures leads to a conclusion that injectors and producers may link very early in a waterflood. Consequently, we expand our prior water injection model to include a hydrofracture that intersects multiple reservoir layers. In some layers, steady-state flow develops between the injector and neighboring producers.

As in Ref. 5, here we consider slow growth of the hydrofracture during water injection, rather than a spur fracture extension during an initial fracturing job. Our analysis involves only the volumetric balance of injected and withdrawn fluids. We do not try to calculate the shape or the orientation of hydraulic fracture from rock mechanics because they are not needed here.

The control procedure is designed in the following way. First, the desirable goal of cumulative injection (or, equivalently, injection rate) is determined. This decision can be made from a waterflood analysis,[1] reservoir simulation, and economic considerations. Second, by analyzing the deviation of actual cumulative injection from the target cumulative injection, and using the estimated frac-

This paper (SPE 71751) was revised for publication from paper SPE 59300, first presented at the 2000 SPE/DOE Improved Oil Recovery Symposium, Tulsa, 3–5 April. Original manuscript received for review 11 April 2000. Revised manuscript received 13 February 2001. Manuscript peer approved 27 February 2001.

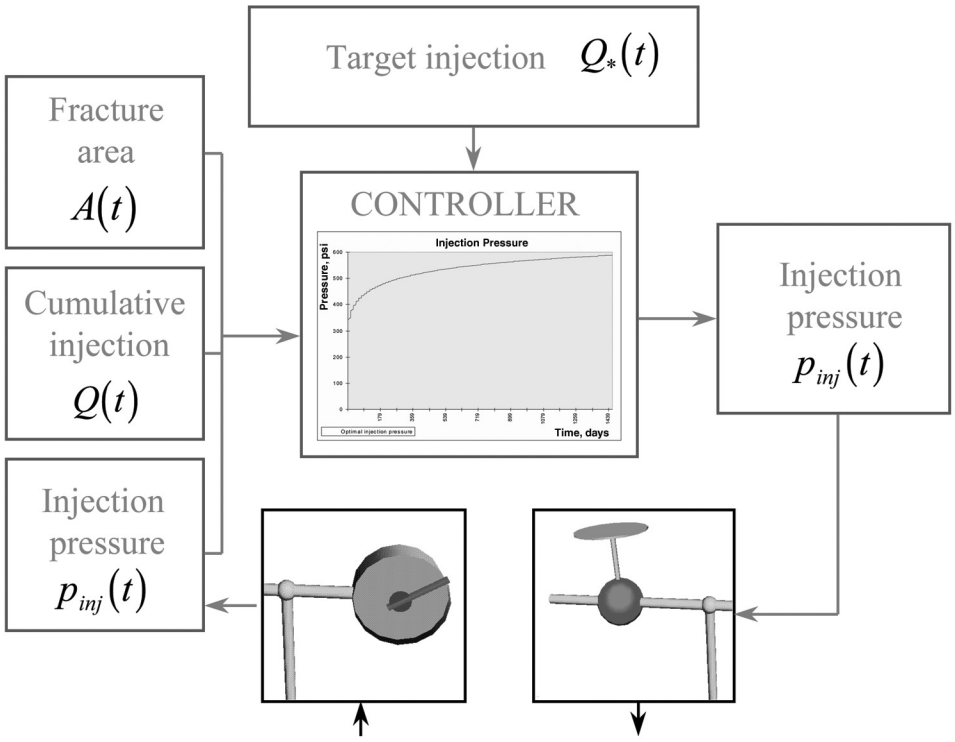

Fig. 1—The controller schematic.

ture area, the controller determines the injection pressure, which minimizes this deviation. Control is applied by adjusting a flow valve at the wellhead, and it is iterated in time (Fig 1).

The convolution nature of the model prevents us from obtaining the optimal solution as a genuine feedback control and designing the controller as a standard closed-loop system. At each timestep, we have to account for the previous history of injection. However, the feedback mode may be imitated by designing the control on a relatively short interval that slides with time. When an unexpected event happens (e.g., a sudden fracture extension occurs), a new sliding interval is generated and the controller is refreshed.

Our controller is process model-based. Although we cannot yet predict when and how the fracture extensions occur, the controller automatically takes into account the effective fracture area changes and the decline of the pressure gradient caused by gradual saturation of the surrounding formation with injected water. The concept of effective fracture area implicitly accounts for the change of rock permeability in the course of operations.

This paper is organized as follows. First, we review a modified Carter's model of transient water injection from a growing hydrofracture. Second, we extend this model to incorporate the case of layered formation with possible channels or thief-layers. Third, we illustrate the model by several field examples. Fourth, we formulate the control problem and present a system of equations characterizing optimal injection pressure. We briefly elaborate on how this system of equations can be solved for different models of hydrofracture growth. A more detailed exposition can be found in Ref. 5. Finally, we extend our analysis of the control model to the case of layered reservoir with steady-state flow in one or several layers.

Modified Carter's Model

We assume transient linear flow from a vertical hydrofracture through which a slightly compressible fluid (water) is injected perpendicularly to the fracture plane, into the surrounding uniform rock of low permeability. The fluid is injected under a uniform pressure, which depends on time. In this context, "transient" means that the pressure distribution in the formation is changing with time (e.g., maintaining a constant injection rate requires variable pressure). Under these assumptions, the cumulative injection can be calculated from the following equation[4,5]:

$$Q(t) = wA(t) + 2\frac{kk_{rw}}{\mu_w\sqrt{\pi\alpha_w}}\int_0^t \frac{\left[p_{\text{inj}}(\tau) - p_i\right]A(\tau)}{\sqrt{t-\tau}}dt\,. \quad \ldots\ldots (1)$$

Here, k and k_{rw}=respectively the absolute rock permeability and the relative water permeability in the formation outside the fracture, and μ_w=the water viscosity. Parameters α_w and p_i=the hydraulic diffusivity and the initial pressure in the formation, repectively. The effective fracture area at time t is measured as $A(t)$, and its constant width is denoted by w. Thus, the first term on the right side of Eq. 1 represents the volume of injected fluid necessary to fill the fracture. This volume is small in comparison with the second term. We assume that the permeability inside the hydrofracture is much higher than the surrounding formation permeability, so at any time the pressure drop along the fracture is negligibly small. We introduce $A(t)$ as an effective fracture area because, first, in a soft rock, the hydrofracture is not a plane crack, but a complex 3D volume; second, the formation permeability changes because of progressing rock damage; and, finally, the water-phase permeability may change with time due to formation plugging and increasing water saturation.[11] In addition, the injected water may not fill the entire fracture volume. Therefore, in general, $A(t)$ is not equal to the geometric area of the hydrofracture.

From Eq. 1 it follows that the initial value of the cumulative injection is equal to $wA(0)$. The control objective is to keep the injection rate, $q(t)$, as close as possible to a prescribed target injection rate, $q_*(t)$. Because Eq. 1 is formulated in terms of cumulative injection, it is more convenient to formulate the optimal control problem in terms of target cumulative injection:

$$Q_*(t) = Q_*(0) + \int_0^t q_*(\tau)\,d\tau\,. \quad \ldots\ldots\ldots\ldots\ldots\ldots\ldots (2)$$

If control maintains the actual cumulative injection close to $Q_*(t)$, then the actual injection rate is close to $q_*(t)$ on average.

Carter's Model for Layered Reservoirs

We assume transient linear flow from a vertical hydrofracture injecting an incompressible fluid into the surrounding formation. The flow is perpendicular to the fracture faces. The reservoir is layered and there is no crossflow between the layers. We also assume

that the initial pressure distribution is hydrostatic. The vertical pressure variation inside each layer is neglected. We can denote by N the number of layers and let h_i, $i=1,2,\ldots,N$, be the thickness of each layer. The area of the fracture in layer i is equal to

$$A_i(t) = a_i \frac{h_i}{h_t} A(t), \quad \ldots\ldots\ldots\ldots\ldots\ldots\ldots\ldots\ldots\ldots (3)$$

where h_t=the total thickness of injection interval: $h_t = \sum_{j=1}^{N} h_j$, and a_i denotes a dimensionless coefficient characterizing fracture propagation in layer i. In those layers where the fracture propagates above average, we have $a_i>1$, whereas where the fracture propagates less, we have $a_i<1$. Clearly, the following condition is satisfied.

$$\sum_{i=1}^{N} a_i h_i = h_t. \quad \ldots\ldots\ldots\ldots\ldots\ldots\ldots\ldots\ldots\ldots (4)$$

The injected fluid pressure, $p_{\text{inj}}(t)$, depends on time t. If the permeability and the hydraulic diffusivity of layer i are equal, respectively, to k_i and α_{wi}, then cumulative injection into layer i is given by the following equation.[4,5]

$$Q_i(t) = wA_i(t) + 2\frac{k_i k_{rw_i}}{\mu_w \sqrt{\pi \alpha_w}} \int_0^t \frac{\left(p_{\text{inj}}(\tau) - p_{\text{init}}\right) A_i(\tau)}{\sqrt{t-\tau}} d\tau. \quad \ldots\ldots (5)$$

Eq. 5 is valid only in layers with transient flow. The layers where steady-state flow has been established must be treated differently. Note that in general the relative permeabilities, k_{rw_i}, may vary in different layers. By assumption, the difference $p_{\text{inj}} - p_{\text{init}}$ is the same in all layers. Summed up for all i, and with Eq. 3, Eq. 5 implies:

$$Q(t) = wA(t) + 2\frac{\bar{k}}{\mu_w \sqrt{\pi}} \int_0^t \frac{\left[p_{\text{inj}}(\tau) - p_{\text{init}}\right] A(\tau)}{\sqrt{t-\tau}} d\tau, \quad \ldots\ldots\ldots\ldots\ldots\ldots\ldots (6)$$

where

$$\bar{k} = \frac{1}{h_t} \sum_{i=1}^{N} a_i h_i \frac{k_i k_{rw_i}}{\sqrt{\alpha_{wi}}} \quad \ldots\ldots\ldots\ldots\ldots\ldots\ldots\ldots\ldots\ldots (7)$$

is the thickness- and hydraulic-diffusivity-averaged reservoir permeability. Note that an increase of the layer permeability, k_i, has the same effect as an increase of the coefficient a_i.

From Eqs. 5 through 7 it follows that the portion of injected water entering layer i is

$$Q_i(t) = \frac{wa_i h_i}{h_t} A(t) + \frac{k_i k_{rw_i} a_i h_i}{\mu_w \sqrt{\alpha_{wi}} h_t} \int_0^t \frac{\left[p_{\text{inj}}(\tau) - p_{\text{init}}\right] A(\tau)}{\sqrt{t-\tau}} d\tau. \quad \ldots\ldots\ldots (8)$$

Now, assume that all N layers fall into two categories. The layers with indices $i \in I = \{i_1, i_2, \ldots, i_T\}$ are in transient flow, whereas the layers with indices $j \in J = \{j_1, j_2, \ldots, j_S\}$ are in steady-state flow (i.e., a connection between the injector and producers has been established). From Eq. 8 we infer that the total cumulative injection into transient-flow layers is

$$Q_I(t) = \sum_{i \in I} \frac{wa_i h_i}{h_t} A(t) + \sum_{i \in I} \frac{k_i k_{rw_i} a_i h_i}{\mu_w \sqrt{\alpha_{wi}} h_t} \int_0^t \frac{\left[p_{\text{inj}}(\tau) - p_{\text{init}}\right] A(\tau)}{\sqrt{t-\tau}} d\tau. \quad \ldots\ldots\ldots (9)$$

By definition, the sets of indices I and J are disjoint and together yield all the layer indices $\{1,2,\ldots,N\}$. It is natural to assume that the linkage is first established in the layers with highest permeability.

$$\min_{j \in J} \left(kk_{rw}\right)_j > \max_{i \in I} \left(kk_{rw}\right)_i. \quad \ldots\ldots\ldots\ldots\ldots\ldots\ldots\ldots\ldots (10)$$

The flow rate in each layer from set J is given by

$$q_j(t) = \frac{k_j k_{rw_j} A_j(t)}{\mu_w} \frac{p_{\text{inj}}(t) - p_{\text{pump}}(t)}{L_j}, \quad \ldots\ldots\ldots\ldots\ldots\ldots (11)$$

where L_j=the distance between the injector and its neighboring producer linked through layer j, and $p_{pump}(t)$=the downhole pressure at the producer. Here, for simplicity, we assume that all flow paths on one side of the hydrofracture connect the injector under consideration to one producer. The total flow rate into the steady-state layers is

$$q_J(t) = \left[p_{\text{inj}}(t) - p_{\text{pump}}(t)\right] A(t) \sum_{j \in J} \frac{k_j k_{rw_j} a_j h_j}{\mu_w h_t L_j}. \quad \ldots\ldots\ldots (12)$$

Because circulation of water from an injector to a producer is not desirable, we come to the following requirement: $q_J(t)$ should not exceed an upper admissible bound q_{adm}: $q_J(t) \le q_{\text{adm}}$. Evoking Eq. 12, one infers that the following constraint is imposed on the injection pressure:

$$p_{\text{inj}}(t) \le p_{\text{adm}}(t), \quad \ldots\ldots\ldots\ldots\ldots\ldots\ldots\ldots\ldots\ldots (13)$$

where the admissible pressure $p_{\text{adm}}(t)$ is given by

$$p_{\text{adm}}(t) = p_{\text{pump}}(t) + \frac{q_{\text{adm}}}{A(t) \sum_{j \in J} \frac{k_j k_{rw_j} a_j h_j}{L_j \mu_w h_t}}. \quad \ldots\ldots\ldots\ldots (14)$$

Eq. 14 leads to an important conclusion. Earlier we have demonstrated that injection into a transient-flow layer is determined by a convolution integral of the product of the hydrofracture area and the difference between the injection pressure and initial formation pressure. In transient flow, water injection rate does increase with the injector hydrofracture area, but water production rate does not. In contrast, from Eqs. 12 and 14, it follows that as soon as linkage between an injector and producer occurs, a larger fracture area and/or more rock damage increase the rate of water recirculation from the injector to the producer. At the initial transient stage of waterflood, a hydrofracture plays a positive role; it helps to maintain higher injection rate and push more oil towards the producing wells. With channeling, the role of the hydrofracture is reversed. The larger the hydrofracture area, the more water is circulated between injector and producers. As our analysis of actual field data shows, channeling is almost inevitable, sometimes at remarkably early stages of waterflood. Therefore, it does matter how the initial hydrofracturing job is done and how the waterflood is initiated. An injection policy that is too aggressive will result in a fast start of injection, but may cause severe problems later on, sometimes very soon. The restriction imposed by Eq. 14 on admissible injection pressure is more severe for a low-permeability reservoir with soft rock. In such a reservoir, there are no brittle fractures, but rather an ever-increasing rock damage, which converts the rock into a pulverized "process zone." At the same time, well spacing in low-permeability reservoirs can be as small as 50 ft between the wells. Both these factors cause the admissible pressure in Eq. 14 to be less.

Field Examples

In this section, we illustrate the model of simultaneous transient and steady-state flow by several examples. We assume that some of the relevant parameters do not vary in time arbitrarily, but are piecewise constant. Although such an assumption may not be valid in some situations, the field examples below show that the calculations match the data quite well and that the assumption is apparently fulfilled.

Let us consider a situation where the injection pressure, the hydrofracture effective area, and the effective cross-sectional area of flow channels are piecewise constant functions of time. We also assume that the pump pressure at the linked producer is also a piecewise constant function of time. In fact, for the conclusions below it is sufficient that the aggregated parameters

$$Y(t)=\sum_{j\in J}\frac{k_j k_{rw_j} a_j h_j}{\mu_w L_j h_t}\left[p_{\text{inj}}(t)-p_{\text{pump}}(t)\right]A(t)$$

and $$Z(t)=\sum_{i\in I}\frac{k_i k_{rw_i} a_i h_i}{\mu_w\sqrt{\alpha_{wi}}\,h_t}\left[p_{\text{inj}}(\tau)-p_{\text{init}}\right]A(t) \quad \ldots\ldots\ldots\ldots (15)$$

are piecewise constant functions of time, whereas individual terms in Eq. 15 can vary arbitrarily. Let t=cumulative time measured from the beginning of observations, and denote by

$$0=\theta_0<\theta_1<\theta_2<\ldots, \quad \ldots\ldots\ldots\ldots\ldots\ldots\ldots\ldots (16)$$

the time instants when either $Y(t)$ or $Z(t)$ changes its value. Furthermore, let Y_i and Z_i=the values which functions $Y(t)$ and $Z(t)$, respectively, take on in the interval $[\theta_{i-1},\theta_i]$, $i=1,2,...$ Then, from Eqs. 9 and 12, the cumulative injections into the transient-flow (Q_T) and steady-state-flow (Q_S) layers are given by the following equations:

$$Q_S(t)=\sum_{i>0}Y_i\left[(t-\theta_{i-1})_+-(t-\theta_i)_+\right]$$

and $$Q_T(t)=\sum_{i>0}Z_i\left[\sqrt{(t-\theta_{i-1})_+}-\sqrt{(t-\theta_i)_+}\right], \quad \ldots\ldots\ldots\ldots (17)$$

where $(t)_+=\max\{0,t\}$. In Eq. 17, we neglect the volume of liquid residing inside the hydrofracture itself. Thus, for the total cumulative injection we get

$$Q(t)=Q_T(t)+Q_S(t)$$
$$=\left\{\begin{matrix}Y_i\left[(t-\theta_{i-1})_+-(t-\theta_i)_+\right]\\ +Z_i\left[\sqrt{(t-\theta_{i-1})_+}-\sqrt{(t-\theta_i)_+}\right]\end{matrix}\right\}. \quad \ldots\ldots\ldots\ldots (18)$$

Note that only the terms where $\theta_i<t$ are nonzero in Eqs. 17 and 18, so that, for instance,

$$Q_S(t)=Y_1 t \text{ and } Q_T(t)=Z_1\sqrt{t} \text{ for } 0<t<\theta_1. \quad \ldots\ldots\ldots\ldots (19)$$

The ratio between Y_i and Z_i measures the distribution of the injected liquid between transient and steady-state layers. If $Y_i \gg Z_i$, then the injection is mostly transient. If, conversely, $Y_i \ll Z_i$, the flow is mostly steady-state, and waterflooding is reduced essentially to water circulation between injectors and producers. The value

$$T_i=\left(\frac{Z_i}{Y_i}\right)^2 \quad \ldots\ldots\ldots\ldots\ldots\ldots\ldots\ldots\ldots\ldots (20)$$

has the dimension of time. It has the following meaning. In the sum $Yt+Z\sqrt{t}$, which characterizes the distribution of the entire flow between steady-state and transient flow regimes, at early times the square root term dominates. Later on, both terms equalize, and at still larger t the linear term dominates. The ratio in Eq. 20 provides a characteristic time of this transition and it can be used as a criterion to distinguish between the flow regimes.

If additional information about the hydrofracture size, reservoir, hydrofracture layers, absolute and relative permeabilities of individual layers, bottomhole injection and production pressures, and initial formation pressure, etc., were available, further quantitative analysis could be performed based on Eqs. 9, 12, and 15. Here we perform estimates of the aggregated coefficients (as seen in Eq. 15) only.

If one considers

$$\psi_{S,i}(t)=(t-\theta_{i-1})_+-(t-\theta_i)_+$$

$$\psi_{T,i}(t)=\sqrt{(t-\theta_{i-1})_+}-\sqrt{(t-\theta_i)_+}, \; i=1,2,\ldots, \quad \ldots\ldots\ldots (21)$$

then from Eq. 18 it follows that

$$Q(t)=\sum_{i>0}\left[Y_i\psi_{S,i}(t)+Z_i\psi_{T,i}(t)\right]. \quad \ldots\ldots\ldots\ldots\ldots (22)$$

If a well is equipped with a flow meter, then coefficients Y_i and Z_i can be estimated to match the measured cumulative injection curve with the calculated cumulative injection using Eqs. 21 and 22. Mathematically, it means solving a system of linear equations with respect to Y_i, Z_i implied by minimum of the following quadratic target function.

$$F=\frac{1}{N}\sum_{n=1}^{N}\left\{Q_M(t_n)-\sum_{i>0}\left[Y_i\psi_{S,i}(t_n)+Z_i\psi_{T,i}(t_n)\right]\right\}^2. \quad \ldots\ldots (23)$$

Here t_1, t_2, etc.,=the measurement times. The instants of time θ_i, as in Eq. 18, can be selected based on the information about the injection pressure and the jumps of injection rate.

Several water injectors in a diatomaceous oil field in California have been analyzed for the flow regimes. In **Figs. 2 through 10,** we present examples of cumulative injection matches. In each case, we selected three values, θ_1 through θ_3, and obtained good fits of the field data. The time intervals are different for different wells according to the availability of data. The calculated coefficients Y_i, Z_i are listed in **Table 1,** and the characteristic times, as seen in Eq. 20, in **Table 2.** Matching the cumulative injection at early times is problematic because there is no information about well operation before the beginning of the sampled interval. From Eq. 9, it is especially true for wells with large hydrofractures. This explains why Z_1 is negative for Wells A and C. The negative value of Y_4 for Well B cannot be interpreted this way, but the magnitude $|Y_4|$ is about 0.25% of the value of $|Z_4|$, well below the accuracy of the measurements, so Y_4 is equal to zero. Comparative analysis of the three wells leads to the following conclusions. Well A (Figs. 2 through 4) has the lowest values of the characteristic times (Eq. 20) in all three time intervals, and demonstrates behavior typical for a well with steady-state flow. Apparently, a major breakthrough occurred at an early time, and a large portion of the injected water was circulated between this injector and the neighboring producers. Conversely, Well B (Figs. 5 through 7) demonstrates a typical transient-flow behavior. However, the growth of Z_i from early to later times indicates that the hydrofracture could experience dramatic extensions at Points 1 and 3 and a moderate extension at Point 2 (Fig. 7). In Well C (Figs. 8 through 10), we recognize transient flow between Points 1 and 3, with a fracture extension at Point 2, Figs. 9 and 10. The small value of T_1 (Table 2) may indicate presence of a small channel, which is later plugged due to the rock damage during fracture extension at Time 1. The decreasing values $T_{2,3,4}$ indicate an increasing steady-state flow component ending up with mostly water recirculation after Time 3.

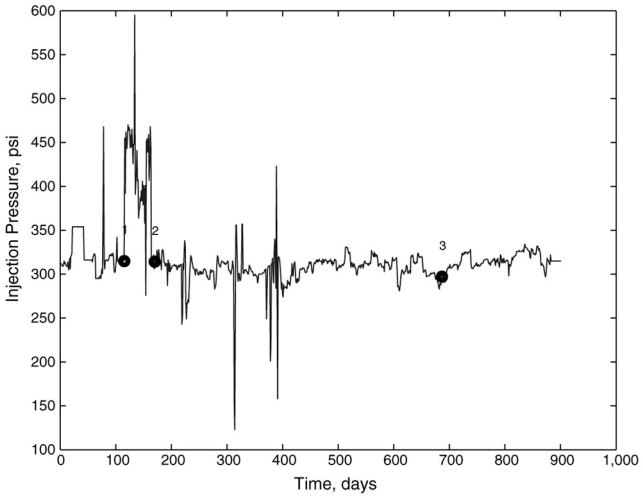

Fig. 2—Well A: Injection pressure.

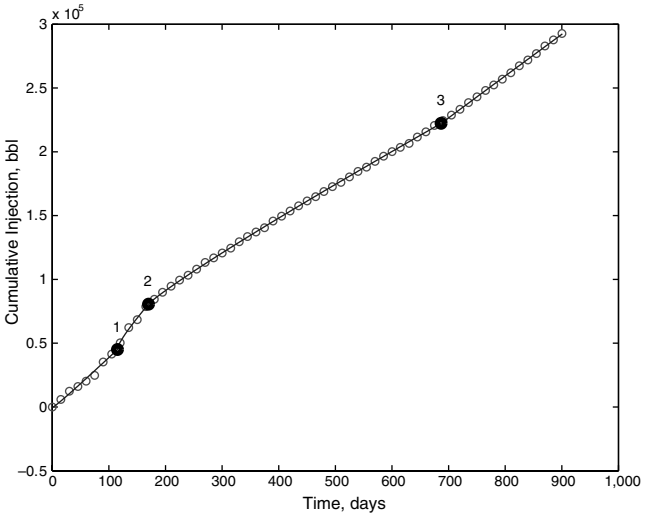

Fig. 3—Well A: Cumulative injection vs. time. Waterflooding is dominated by steady-state linkage with a producer. Circles represent data, the solid line represents computations.

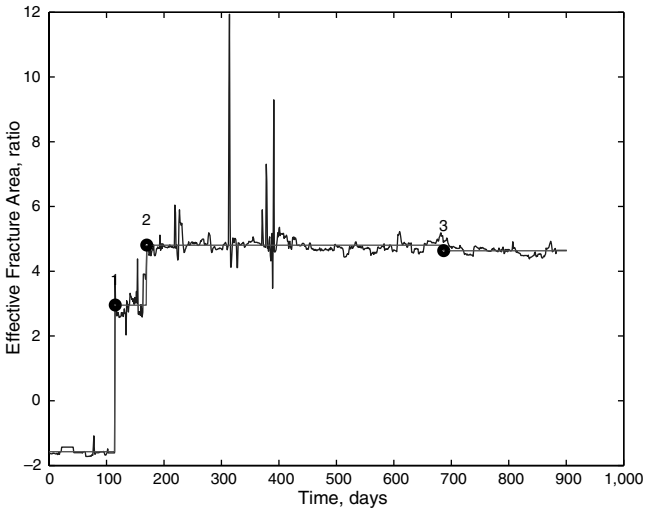

Fig. 4—Well A: Effective fracture area calculated using measured pressures (jagged line) and injection pressures averaged over respective intervals.

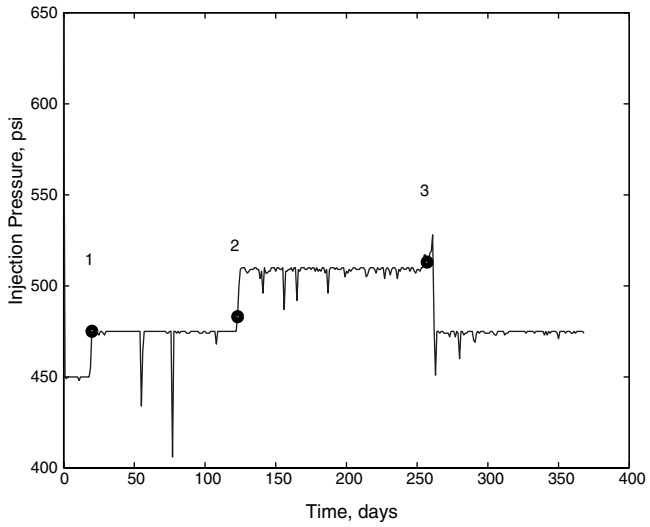

Fig. 5—Measured injection pressures vs. time for Well B.

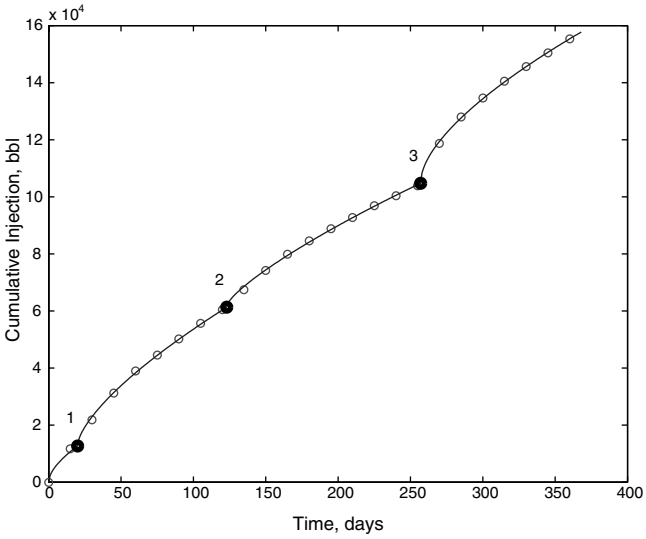

Fig. 6—In Well B, waterflooding is dominated by transient flow with possible hydrofracture extensions. Circles represent data, the solid line represents computations.

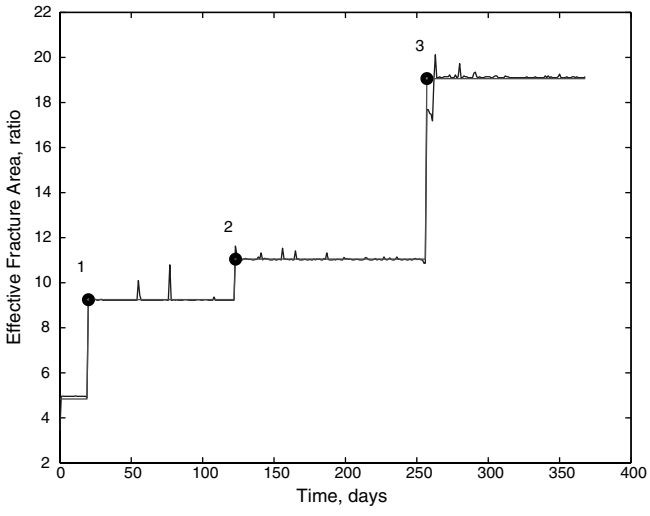

Fig. 7—Well B: Effective fracture area calculated using measured pressures (slightly jagged line) and injection pressures averaged over respective intervals almost coincide.

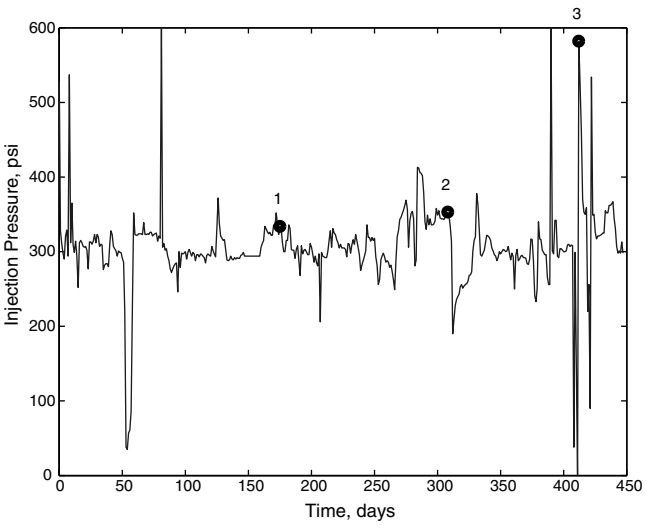

Fig. 8—In Well C, the injection pressure has numerous fluctuations with no apparent behavior pattern.

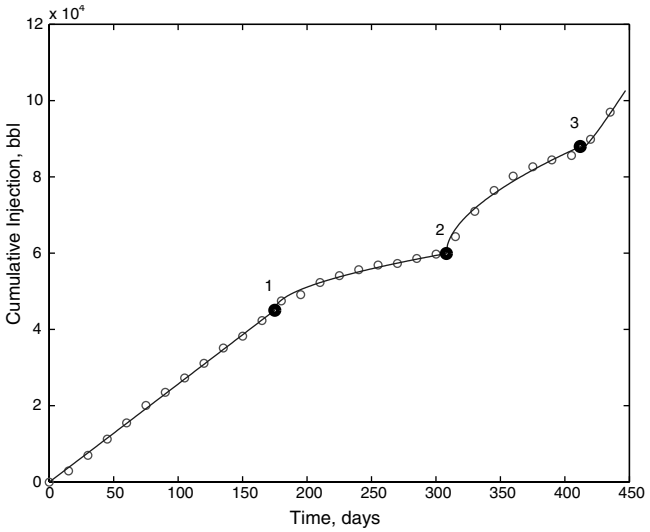

Fig. 9—Well C: Waterflooding has a mixed character where periods of transient flow are alternated with periods of mostly steady-state flow. Circles represent data, the solid line represents computations.

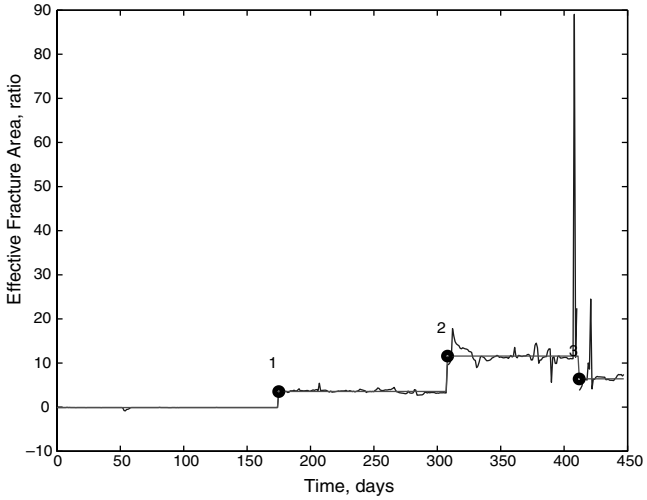

Fig. 10—Well C: Effective fracture area calculated using measured pressures (jagged line) and injection pressures averaged over respective intervals. The zero initial area estimates imply possible linkage with a producer, resulting in mostly steady-state flow.

TABLE 1—LUMPED STEADY-STATE AND TRANSIENT FLOW PARAMETERS FOR WATER INJECTION IN THREE EXAMPLE WELLS

Well	Y_1	Y_2	Y_3	Y_4	Z_1	Z_2	Z_3	Z_4
A	438.5	220.8	438.2	298.7	–507.3	1209.1	1468.4	1462.9
B	139.5	116.0	51.2	–22.7	2229.6	4381.2	5615.7	9073.2
C	259.7	3.1	15.7	480.3	–29.8	1116.8	3383.2	2204.5

TABLE 2—CHARACTERISTIC TRANSITION TIMES BETWEEN TRANSIENT AND STEADY-STATE WATER INJECTION IN THREE EXAMPLE WELLS

Well	T_1 (days)	T_2 (days)	T_3 (days)	T_4 (days)
A	1.3384	29.9865	11.2291	23.9861
B	255.4	1426.5	12030.1	159760.4
C	0.013	129785.9	46436.1	21.07

Control Model

To formulate the optimal control problem, we must choose a performance criterion for the process described by Eq. 1. Suppose that we are planning to apply control on a time interval $[\theta,T]$, where $T>\theta\geq 0$. In particular, we assume that the cumulative water injection and the injection pressure are known on interval $[0,\theta]$, along with the effective fracture area $A(t)$. On interval $[\theta,T]$, we want to apply such an injection pressure that the resulting cumulative injection will be as close as possible to that given by Eq. 2. This requirement may be formulated as follows.

Minimize

$$J\left[p_{inj}\right]=\frac{1}{2}\int_{\theta}^{T}w_q(t)\left[Q(t)-Q_*(t)\right]^2dt$$

$$+\frac{1}{2}\int_{\theta}^{T}w_p(t)\left[p_{\text{inj}}(t)-p_*(t)\right]^2dt, \quad \ldots\ldots\ldots\ldots\ldots (24)$$

subject to constraint given by Eq. 1.

The weight-functions w_p and w_q are positive. They reflect the tradeoff between the closeness of actual cumulative injection $Q(t)$ to the target $Q_*(t)$, and the well-posedness of the optimization problem. For small values of w_p, minimization of Eq. 24 forces $Q(t)$ to follow the target injection strategy, $Q_*(t)$. However, if w_p is too small, then the problem of minimization of Eq. 24 becomes ill-posed.[12,13] Moreover, the function w_p is in a denominator in Eq. 26 below, which characterizes the optimal control. Therefore, computational stability of this criterion deteriorates as w_p approaches zero. At the same time, if we consider a specific mode of control (e.g., piecewise constant control), then the well-posedness of the minimization problem is not affected by $w_p\equiv 0$.[14] Function $p_*(t)$ defines a stabilizing value of the injection pressure. Theoretically, this function can be selected arbitrarily; however, practically speaking, it should be a rough estimate of the optimal injection pressure. Below, we discuss the ways in which $p_*(t)$ can be reasonably specified.

The optimization problem we just have formulated is a linear-quadratic optimal-control problem. In the next section, we present the necessary and sufficient conditions of optimality in the form of a system of integral equations.

Optimal Injection Pressure

Here we analyze the necessary and sufficient optimality conditions for the minimum of the criterion (Eq. 24) subject to constraint (Eq. 1). We briefly characterize optimal control in two different modes: the continuous mode and the piecewise-constant mode. In addition, we characterize the injection-pressure function, which provides exact identity $Q(t)\equiv Q_*(t)$, where $\theta\leq t\leq T$. A more detailed exposition is presented in Ref. 14. In particular, we have deduced that the optimal injection pressure and the cumulative injection policy on time interval $[\theta:T]$ are obtained by solving the following system of integral equations.[14]

$$Q_0(t)=wA(t)$$

$$+2\frac{kk_{rw}}{\mu_w\sqrt{\pi\alpha_w}}\int_0^{\theta}\frac{\left[p_{\text{inj}}(\tau)-p_i\right]A(\tau)}{\sqrt{t-\tau}}d\tau$$

$$+2\frac{kk_{rw}}{\mu_w\sqrt{\pi\alpha_w}}\int_{\theta}^{t}\frac{\left[p_0(\tau)-p_i\right]A(\tau)}{\sqrt{t-\tau}}d\tau, \quad \ldots\ldots\ldots\ldots (25)$$

and

$$p_0(t)=p_*(t)$$

$$-2\frac{kk_{rw}}{\mu_w\sqrt{\pi\alpha}w_p(t)}A(t)\int_t^T\frac{w_q(\tau)}{\sqrt{\tau-t}}\left[Q_0(\tau)-Q_*(\tau)\right]d\tau. \quad \ldots\ldots\ldots\ldots\ldots\ldots\ldots\ldots (26)$$

The importance of a nonzero weight function, $w_p(t)$, is now obvious. If this function vanishes, the injection pressure cannot be calculated from Eq. 26 and the controller output is not defined. The properties of the system of integral equations (Eqs. 25 and 26) are further discussed in Ref. 14.

Eq. 26, in particular, implies that the optimal injection pressure satisfies the condition $p_0(T)=p_*(T)$. The trivial function $p_*(t)\equiv 0$ is not a good choice of the reference pressure in Eq. 24 because it enforces zero injection $p_*(t)$ pressure by the end of the current subinterval. Another possibility, $p_*(t)\equiv p_{init}$ has the same drawback: it equalizes the injection pressure and the pressure outside the fracture by the end of the current interval. Apparently $p_*(t)$ should exceed p_i for all t. At the same time, too high a value of $p_*(t)$ is not desirable, because it may cause a catastrophic extension of the fracture. A rather simple and reasonable choice of $p_*(t)$ is provided by $p_*(t)\equiv P_*$, where P_* is the optimal constant pressure on the interval. The equation characterizing P_* is obtained in Ref. 14. As soon as we have selected the target stabilizing function, $p_*(t)$, the optimal injection pressure is provided by solving Eqs. 25 and 26.

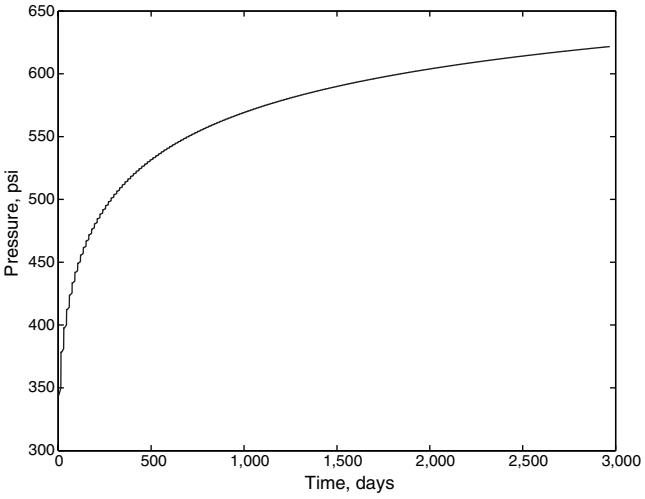

Fig. 11-Optimal injection pressure when hydrofracture grows as the square root of time.

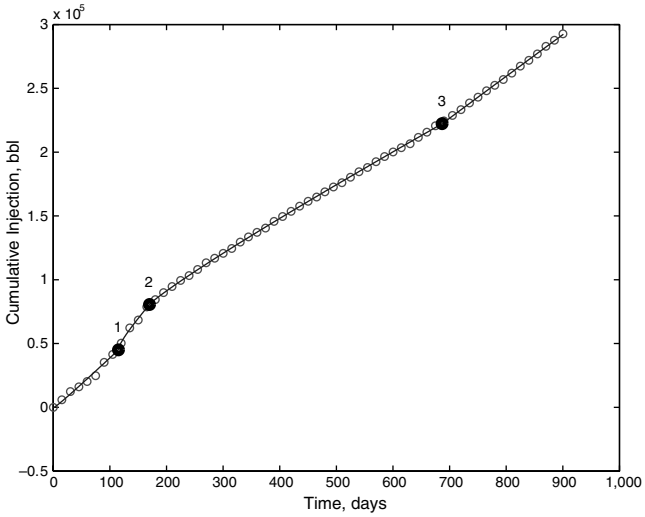

Fig. 13—Three modes of optimal pressure when fracture area is measured with delay and random disturbances while the fracture experiences extensions (see Fig. 14). The jagged line plots exact optimal pressure, the solid line plots piecewise constant optimal pressure, and the dashed line plots the optimal pressure obtained by solving a system of Eqs. 25 and 26.

Note that the optimal injection pressure depends on effective fracture area, $A(t)$, and on the deviation of the cumulative injection, $Q_0(t)$, from the target injection, $Q_*(t)$, measured on the entire interval $[0,T]$, rather than on the current instantaneous values. Thus, Eq. 26 excludes genuine feedback-control mode.

There are several ways to circumvent this difficulty. First, we can organize the process of control as a systematic procedure. We split the whole-time interval into reasonably small parts, so that on each part one can make reasonable estimates of the required parameters. Then we compute the optimal injection pressure for this interval and apply it by adjusting the control valve. As soon as either the measured cumulative injection or the effective fracture area begins to deviate from the estimates used to determine the optimal injection pressure, the control interval $[\theta,T]$ is refreshed. We must also revise our estimate of the fracture area, $A(t)$, for the refreshed interval and the expected optimal cumulative injection. In summary, the control is designed on a sliding time interval $[\theta,T]$. The control interval should be refreshed before the current interval ends even if the measured and computed parameters are in good agreement. Computer simulations show, in **Figs. 11 through 14**, that an overlap of control intervals results in an appropriate reaction of the controller to the changing injection conditions.

Another possibility to resolve the difficulty in obtaining the optimal control from Eq. 26 is to change the model of fracture

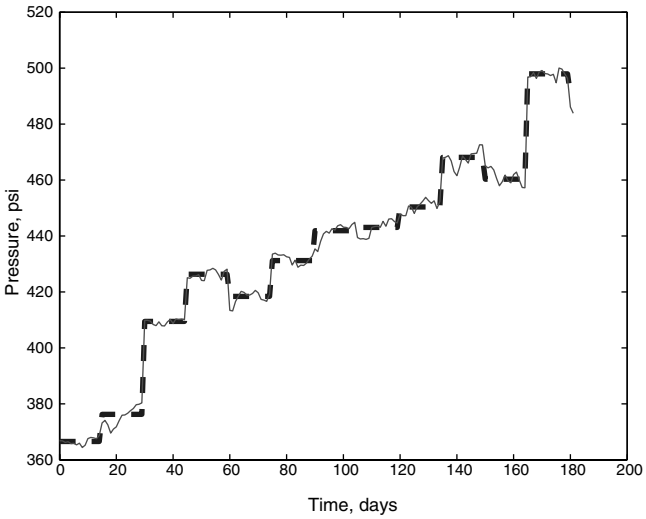

Fig. 12—Optimal (solid line) and piecewise-constant (dashed line) injection pressures if fracture area is estimated with random disturbances.

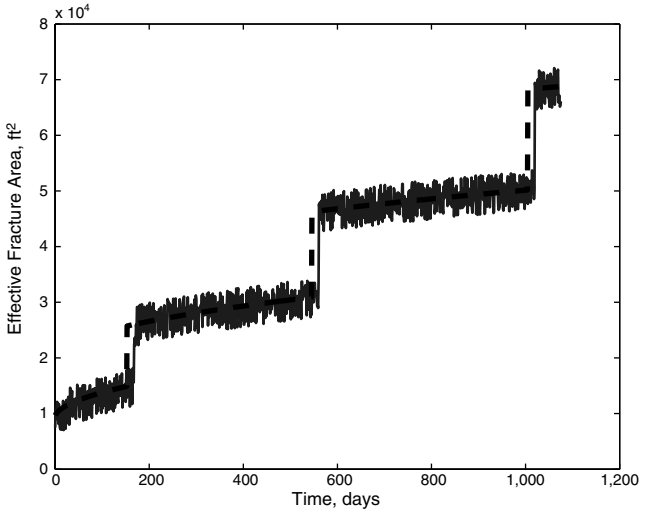

Fig. 14—Fracture growth with several extensions (dashed line). The hydrofracture area is measured with random noise and delay (jagged line).

growth. So far, we have treated the fracture as a continuously growing object. On the other hand, it is clear that the rock surrounding the fracture is not perfect, and the area of the fracture grows in steps. This observation leads to the piecewise-constant fracture growth model. We may assume that the fracture area is constant on the current interval $[\theta,T]$. If observation tells us that the fracture area has changed, the interval $[\theta,T]$ must be adjusted, and control refreshed. Eqs. 25 and 26 are simpler for piecewise constant fracture area.[14]

Control Model for a Layered Reservoir

Now let us consider a control problem in the situation where there is a water breakthrough in one or more layers of higher permeability. From Eq. 6 the total injection into the transient layers is given by

$$Q_T(t) = wA_T(t) + 2\frac{K_T}{\mu_w\sqrt{\pi}}\int_0^t \frac{\left[p_{\text{inj}}(\tau)-p_{\text{init}}\right]A(\tau)}{\sqrt{t-\tau}}d\tau, \quad \ldots\ldots\ldots\ldots (27)$$

where

$$A_T(t) = \frac{1}{h_t}\sum_{i\in I} a_i h_i A(t)$$

and $$K_T = \frac{1}{h_t}\sum_{i\in I} h_i \frac{a_i k_i k_{rw_i}}{\sqrt{\alpha_{wi}}}. \quad \ldots\ldots\ldots\ldots\ldots\ldots\ldots\ldots (28)$$

To estimate the largest possible injection on interval $[\theta,T]$ under constraint (Eq. 13), let us substitute Eq. 13 into Eq. 27:

$$Q_T^{\max}(t) = wA_T(t) + 2\frac{K_T}{\mu_w\sqrt{\pi}}\left\{\int_0^\theta \frac{\left[p_{\text{inj}}(\tau)-p_{\text{init}}\right]A(\tau)}{\sqrt{t-\tau}}d\tau + \int_\theta^T \frac{\left[p_{\text{adm}}(\tau)-p_{\text{init}}\right]A(\tau)}{\sqrt{t-\tau}}d\tau\right\}. \quad \ldots\ldots\ldots\ldots (29)$$

From Eq. 14, one obtains

$$Q_T^{\max}(t) = wA_T(t) + 2\frac{K_T}{\mu_w\sqrt{\pi}}\int_0^\theta \frac{\left[p_{\text{inj}}(\tau)-p_{\text{init}}\right]A(\tau)}{\sqrt{t-\tau}}d\tau + 2\frac{K_T}{\mu_w\sqrt{\pi}}\int_\theta^t \frac{\left[p_{\text{pump}}(\tau)-p_{\text{init}}\right]A(\tau)}{\sqrt{t-\tau}}d\tau + 4\frac{\sum_{i\in I}\frac{k_i k_{rw_i} a_i h_i}{\sqrt{\alpha_{wi}}}}{\sum_{j\in J}\frac{k_j k_{rw_j} a_j h_j}{L_j}} q_{\text{adm}}\sqrt{t-\theta}. \quad \ldots\ldots\ldots\ldots (30)$$

Now let us analyze the right side of Eq. 30. The first term expresses the fraction of the fracture volume that intersects the transient layers. Because the total volume of the fracture is small, this term is also small. The second term decays as $\sqrt{\theta/t}$, so if steady-state flow has been established by time θ the impact of this term is small as $t \gg \theta$. The main part of cumulative injection over a long time interval comes from the last two terms. Because production is possible only if

$$p_{\text{pump}}(\tau) < p_{\text{init}}, \quad \ldots\ldots\ldots\ldots\ldots\ldots\ldots\ldots\ldots\ldots (31)$$

the third term is negative. Therefore, successful injection is possible without exceeding the admissible rate of injection into steady-state layers only if

$$2\frac{K_T}{\sum_{j\in J}\frac{k_j k_{rw_j} a_j h_j}{h_t L_j}} q_{\text{adm}}\sqrt{t-\theta} > \frac{K_T}{\mu_w\sqrt{\pi}}\int_\theta^t \frac{\left[p_{\text{init}} - p_{\text{pump}}(\tau)\right]A(\tau)}{\sqrt{t-\tau}}d\tau. \quad \ldots\ldots\ldots\ldots (32)$$

After linkage has occurred, it is natural to assume that the fracture stops growing, because an increase of pressure will lead to circulating more water to the producers rather than to a fracture extension. In addition, we may assume that producers are pumped off at constant pressure, so that $\Delta p_{\text{pump}} = p_{\text{init}} - p_{\text{pump}}(t)$ does not depend on t. Then, the condition in Eq. 32 transforms into

$$q_{\text{adm}} h_t > \sum_{j\in J}\frac{k_j k_{rw_j} a_j h_j}{\mu_w L_j}\Delta p_{\text{pump}} A_\theta. \quad \ldots\ldots\ldots\ldots\ldots\ldots (33)$$

The latter inequality means that the area of the hydrofracture may not exceed the fatal threshold

$$A_\theta < \frac{q_{\text{adm}} h_t}{\sum_{j\in J}\frac{k_j k_{rw_j} h_j}{\mu_w L_j}\Delta p_{\text{pump}}}. \quad \ldots\ldots\ldots\ldots\ldots\ldots\ldots (34)$$

This conclusion can also be formulated in the following way. In a long run, the rate of injection into the steady-state layers, q_{chnl}, will be at least

$$q_{\text{chnl}} > \frac{1}{h_t}\sum_{j\in J}\frac{k_j k_{rw_j} a_j h_j}{\mu_w L_j}\Delta p_{\text{pump}} A_\theta. \quad \ldots\ldots\ldots\ldots\ldots\ldots (35)$$

Therefore, smaller hydrofractures are better.

A close injector-producer well spacing may increase the amount of channeled water. Indeed, if in Eq. 34 we had $L_j = L$ for all $j \in J$, then the threshold fracture area would be proportional to L, the distance to the neighboring producer. Also, the close injector-producer well spacing makes the rock damage more likely; thus, the layer permeabilities, k_j, increase and the threshold fracture area decreases even further.

Conclusions

In this paper, we have implemented a model of water injection from an initially growing vertical hydrofracture into a layered low-permeability rock. Initially, water injection is transient in each layer. The cumulative injection is then expressed by a sum of convolution integrals, which are proportional to the current and past area of the hydrofracture and the history of injection pressure. In transient flow, therefore, one might conclude that a bigger hydrofracture and higher injection pressure result in more water injection and a faster waterflood. When injected water breaks through in one or more of the rock layers, the situation changes dramatically. Now a larger hydrofracture causes more water recirculation.

We have proposed an optimal controller for transient and transient/steady-state water injection from a vertical hydrofracture into layered rock. We present three different modes of controller operation: the continuous mode, piecewise constant mode, and exact optimal mode. The controller adjusts injection pressure to keep injection rate on target while the hydrofracture is growing. The controller can react to the sudden hydrofracture extensions and the development of injector-producer flow channels, and prevent the catastrophic ones. After water breakthrough occurs in some of the layers, we arrive at a condition for the maximum feasible hydrofracture area, beyond which waterflood may be uneconomic because of excessive recirculation of water.

In summary, we have coupled early transient behavior of water injectors with their later behavior after water breakthrough. We have shown that early water injection policy and the resulting hydrofracture growth may impact very unfavorably the later performance of the waterflood.

Nomenclature

a_i = dimensionless weight coefficients
A = effective fracture area, ft^2
F = fitting criterion for estimating aggregated parameters Y and Z
h_i = thickness of layer i, ft
h_t = total thickness of injection interval, ft
k = absolute rock permeability, md
k_{rw} = relative permeability of water, dimensionless
$\overline{k}$ = average permeability, md
K = the thickness- and hydraulic-diffusivity-averaged reservoir permeability of transient layers, see Eq. 28.
L_i = distance between injector and linked producer in layer i, ft
N = total number of measurement points in fitting criterion F
p_i = initial pressure in the formation outside the fracture, psi
p_{init} = initial pressure
p_{inj} = injection pressure psi
q = volumetric injection rate, bbl/D
q_{chnl} = the rate of injection into the steady-state layers
Q = cumulative injection, bbl
$p_{pump}(t)$ = the downhole pressure at the producer
w = fracture width, in.
w_p, w_q = dimensionless weight coefficient
Y = aggregated parameter characterizing steady-state flow, ft^3/d
Z = aggregated parameter characterizing transient flow, ft^3/d
α = hydraulic diffusivity, ft^2/D
j = porosity, dimensionless
μ = viscosity, cp

Subscripts

adm = admissible
i,j = layers i and j, respectively
I = set of indices of layers i that are in transient flow
M = measured data
S = steady-state flow
T = transient flow
w = water

Acknowledgments

The Assistant Secretary for Fossil Energy, Office of Gas and Petroleum Technology, provided support for this work under contract No. DE-ACO3-76FS00098 to the Lawrence Berkeley Natl. Laboratory of the U. of California. Partial support was provided by two members of the U. of California Oil Consortium, Chevron Petroleum Technology Co., and Aera Energy, LLC.

References

1. De, A. and Patzek, T.W.: "Waterflood Analyzer, MatLab Software Package," Lawrence Berkley National Laboratory, Berkeley, California (1999).
2. Patzek, T.W. and Silin, D.B.: "Use of InSAR in Surveillance and Control of a Large Field Project," 2000 Annual International Energy Agency Workshop and Symposium, Edinburgh, Scotland, 19–22 September.
3. Patzek, T.W.: "Surveillance of South Belridge Diatomite," paper SPE 24040 presented at the 1992 SPE Western Regional Meeting, Bakersfield, California, 30 March–1 April.
4. Patzek, T.W. and Silin, D.B.: "Control of Fluid Injection Into a Low-Permeability Rock—1. Hydrofracture Growth," paper SPE 39698 presented at the 1998 SPE/DOE Improved Oil Recovery Symposium, Tulsa, 19–22 April.
5. Patzek, T.W. and Silin, D.B.: "Water Injection Into a Low-Permeability Rock—1. Hydrofracture Growth," *Transport in Porous Media* (2001) **43,** 537.
6. Holzhausen, G.R. and Gooch, R.P.: "Impedance of Hydraulic Fractures: Its Measurement and Use for Estimating Fracture Closure Pressure and Dimensions," paper SPE/DOE 13892 presented at the 1985 Low Permeability Gas Reservoirs Conference, Denver, Colorado, 19–22 May.
7. Patzek, T.W. and De, A.: "Lossy Transmission Line Model of Hydrofractured Well Dynamics," paper SPE 46195 presented at the 1998 Western Regional Meeting, Bakersfield, California 10–13 May.
8. Ashour, A.A. and Yew, C.H.: "A Study of the Fracture Impedance Method," 1996 CIM Petroleum Society Technical Meeting, Calgary, Canada.
9. Warpinski, N.R.: "Hydraulic Fracture Diagnostics," *JPT* (October 1966) 907.
10. Barenblatt, G.I.: "On the Finiteness of Stresses at the Leading Edge of an Arbitrary Crack," *J. of Applied Mathematics and Mechanics* (1961) **25,** 1112.
11. Barkman, J.H. and Davidson, D.H.: "Measuring Water Quality and Predicting Well Impairment," *JPT* (July 1972) 865.
12. Tikhonov, A.N. and Arsenin, V.Y.: "Solutions of ill-posed problems," *Scripta Series in Mathematics,* J. Fritz (ed.), Halsted Press, New York City (1977).
13. Vasil'ev, F.P.: *Numerical Methods for Solving Extremal Problems,* Nauka Publishing Co., Moscow (1982).
14. Silin, D.B. and Patzek, T.W.: "Water Injection into a Low-Permeability Rock—2. Control Model," *Transport in Porous Media* (2001) **43,** 557.

SI Metric Conversion Factors

bbl × 1.589 873	E − 01 = m^3
cp × 1.0*	E − 03 = Pa•s
D × 8.64*	E + 04 = s
ft × 3.048*	E − 01 = m
ft^2 × 9.290 304*	E − 02 = m^2
in. × 2.54*	E + 00 = cm
md × 9.869	E − 16 = m^2
psi × 6.894 757	E + 00 = kPa

*Conversion factor is exact. **SPEJ**

Dmitriy B. Silin is a geological scientist at the Earth Sciences Div. of Ernest Orlando Lawrence Berkeley Natl. Laboratory. e-mail: Dsilin@lbl.gov. For five years he was an associate professor at M.V. Lomonosov Moscow State U. He holds MS and PhD degrees in applied mathematics from the Dept. of Computational Mathematics and Cybernetics at M.V. Lomonosov Moscow State U. Silin also obtained the degree of Doctor of Physical and Mathematical Sciences in 1993. **Tad W. Patzek** is an associate professor of GeoEngineering at the Dept. of Civil and Environmental Engineering, U. of California, Berkeley. e-mail: patzek@patzek.berkeley.edu. Prior to joining Berkeley, he was a senior reservoir engineer at Shell Western E&P Inc. (1989-90); senior research engineer (1986-89) and research engineer (1983-86) at the Enhanced Recovery Research Dept., Shell Development; research associate at the Chemical Engineering Dept., U. of Minnesota (1981-83); and research associate at Chemical Engineering Research Center, Polish Academy of Sciences, Gliwice, Poland. Patzek has authored 90 papers, 38 industrial reports, and 15 expert witness reports and depositions. In 1995, Patzek was a Distinguished Lecturer for SPE, and he is a member of the SPE Speakers Bureau.